MECHANICAL BEHAVIOUR OF PRESSURE-INFILTRATED CERAMIC PARTICLE REINFORCED ALUMINIUM

M. Kouzeli[1], L. Weber[1], C. San Marchi[1] and A. Mortensen[1]

[1]*Laboratory for Mechanical Metallurgy, Swiss Institute of Technology in Lausanne, CH-1015, Lausanne, Switzerland*

SUMMARY: In an effort to clarify the influence of intrinsic matrix and reinforcement properties on the mechanical behaviour of particle reinforced metal matrix composites, we produced and characterised pure aluminium matrix composites reinforced with about 50 vol. pct Al_2O_3 and B_4C particles (30µm average diameter). Tensile testing of both materials demonstrate elongations to failure on the order of 2.5%, which is high for composites containing 50 vol. pct ceramic. The two materials differ, on the other hand, with regard to the measured ultimate tensile strengths which are about 120 and 200 MPa for the Al_2O_3/Al and B_4C/Al composites, respectively. Internal damage accumulation was monitored via Young's modulus and density decrease measurements. These data are linked to microstructural observations which indicate two distinct damage mechanisms: (i) particle fracture predominant in the Al_2O_3/Al composite, and (ii) nucleation and growth of voids in the matrix of the B_4C/Al composite.

KEYWORDS: infiltrated composites, particle-reinforced aluminium, tensile behaviour, damage evolution, damage mechanisms

INTRODUCTION

Particle reinforced metal matrix composites (PRMMCs) have been the subject of extensive study in the past thirty years due to a need for lightweight structural materials. Even though our understanding of composite mechanical behaviour has progressed significantly over the past decade, the definition of clear strategies for microstructural toughening still remains challenging in part due to the materials studied. In most cases, these are industrially produced engineering materials, featuring complex alloy matrix microstructures, porosity, oxide scale, and/or particle clustering [1-3].

The goal of this study is to contribute to our understanding of fracture and damage mechanisms in PRMMCs by considering a simpler microstructure. To that effect, we characterise the mechanical behaviour of ceramic particle reinforced composites produced by infiltration. These composites contain about 50 vol. pct reinforcement, uniformly distributed throughout the material. Thus the incidence of intrinsic particle and metal constituent characteristics on the mechanical properties of PRMMCs can be put into evidence with greater clarity.

EXPERIMENTAL PROCEDURES

Materials

The matrix of the composites is 99.99% pure aluminium, purchased from VAW (Grevenbroich, Germany). The ceramic reinforcements are alpha-alumina and boron carbide particles, both purchased from Tracomme (Adliswil, Switzerland). They have an angular morphology, and feature an aspect ratio near one with average mean diameter d_{50} = 29.5±1.5 µm.

Free-standing particle beds were packed in closed-end cylindrical alumina crucibles having a nominal inner diameter of 38 mm. Aluminium billets were pre-cast to fit in the alumina crucibles and sufficient aluminium was placed in the crucibles above the powders to fill all the pore space in the preform. After this assembly was inserted into a pressure-infiltration apparatus similar to that described in Ref. [4], the ceramic preforms were evacuated, and the system was subsequently heated to 750°C. Once molten, the metal formed a liquid seal between the powder bed and the furnace atmosphere such that pressurised gas (argon at 8MPa), let into the apparatus, forced the metal into the preform. The composite was then directionally solidified by lowering the crucible onto a copper chill in order to prevent the formation of solidification shrinkage pores within the casting.

Mechanical testing

Tensile tests were conducted according to ASTM Standard B557M-84 on subsized dogbone samples, machined from the pressure-cast composites using electro-discharge machining. A Zwick (Ulm, Germany) 10 kN screw driven tensile testing apparatus was used under displacement control with an initial strain rate of 10^{-4} s^{-1}. Longitudinal strain was measured over a 10mm gauge length using a clip-on extensometer featuring a linearity better than 1µm.

Two testing procedures were used: (i) continuous loading until fracture, and (ii) intermittent unload/reload cycles at predetermined plastic strain increments. The second series of tests were conducted in order to monitor the evolution of Young's modulus and density as a function of composite deformation. Poisson's ratio was also determined for the two composites with the use of precision strain gauges supplied by Measurement Group Inc., Micromeasurements Division (Raleigh, USA).

Microstructural characterisation

The as-cast composites were examined by Scanning Electron Microscopy (SEM) and optical microscopy, using appropriate (uniquely diamond-based) metallographic polishing procedures. For the observation of damage on longitudinal sample sections (*i.e.*, perpendicular to the fracture surface), specimens were electropolished for 5s at 50 V with Struers A2 electrolyte after mechanical polishing, in order to remove the smeared layer of ductile aluminium and to reveal voids within the matrix. This electrolytic polishing step also allows for a distinction between superficial particle cracks caused by polishing, and cracks running through particles that originate from particle failure during tensile testing. Transmission Electron Microscopy (TEM) was also used to characterise the material; to this end standard sample preparation and thinning procedures were used, including ion milling for the final polishing and perforation stages.

Damage evolution

The nucleation and accumulation of damage during tensile straining was monitored independently in two ways: (i) via the evolution of Young's modulus, and (ii) via density measurements.

Tensile modulus measurements
The evolution of the apparent tensile modulus of the material as a function of applied strain was measured on reloading curves after unloading at periodic strain increments. Prior to the

application of standard linear regression techniques to the initial parts of the reload curves, a calculation of the evolution of the local slope was performed in order to determine the most clearly linear region of these curves, if any (incidentally, this did not always coincide with the initial portion of the curve).

In order to determine the uncertainty of the resulting modulus measurements, each unload/reload cycle at each strain increment was repeated at least 3 times. The experimental scatter was never larger than ±0.5%, as represented by the standard deviation of the modulus for each increment.

Density measurement
The composite density after incremental plastic straining was measured using the Ratcliffe method, a differential method for measuring small density changes based on Archimede's principle [5]. The specimen is weighed with respect to a "dummy" sample of the same material in air and in the immersion fluid, both before and after plastic straining. This method has the advantage that close monitoring of temperature is not necessary, because the changes in the weights (in air and immersed) of the dummy sample are used to calibrate temperature variations.

A Sartorius MC 210P microbalance with a sensitivity of ±10μg (IG Instrumenten-Gesellschaft, Zurich, Switzerland) was used, with distilled water as the immersion fluid. By applying this technique, reliable density change measurements on the order of ±0.005% are ensured. Corrections are made for the unstrained volume beyond the shouldered ends of the tensile sample by assuming that all void nucleation occurs in the gauge length. Density measurements of the shouldered ends of a failed tensile sample verified this assumption.

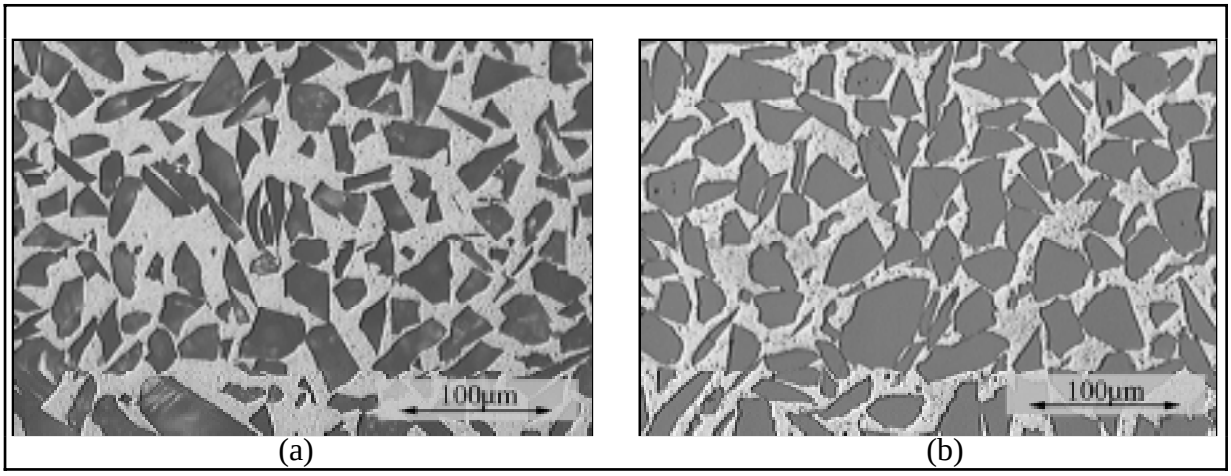

Fig. 1: Optical micrographs of (a) as-cast Al_2O_3/Al composite and (b) as-cast B_4C/Al composite

RESULTS

Microstructure of as-cast composites

Optical metallography of the two as-cast composite systems revealed microstructures characterised by a homogeneous particle distribution and reaction-free particle-matrix interfaces, Fig. 1. Particle volume fractions, measured by image analysis and densitometry, are in the range of 0.48 - 0.52 for both composites. As expected no second phases are observed in the Al_2O_3/Al composite , whereas a small amount of reaction product is found to nucleate and grow on TiB_2 particles which exist as impurities in the B_4C powders prior to infiltration. This reaction product does not seem to influence the integrity of the B_4C/Al interface and was characterised by TEM diffraction techniques as AlB_2. The average size of the AlB_2 particles is less than 20μm and it is estimated by image analysis to account for less than 2% of the composite by volume.

Table 1: Basic mechanical properties of the aluminium matrix composites

Reinforce-ment	Volume fraction, %	Young's Modulus, E_0 (GPa)	Poisson's ratio, ν	Ultimate Tensile Strength, (MPa)	Yield Stress, (MPa)	Engineering strain at failure, %
Al_2O_3	50 ±2	120 ±5	0.28 ±0.01	121 ±2	81 ±2	2.8 ±0.2
B_4C	50 ±2	145 ±5	0.26 ±0.01	197 ±2	140 ±4	2.5 ±0.4

Tensile properties

The incidence of the type of reinforcement on the tensile response of the composites is manifest both in their elastic constants and their plastic flow behaviour. The strength and strain hardening of the B_4C/Al composite are significantly greater than those of the Al_2O_3/Al, while the former is also a stiffer material than the latter.

The tensile properties of the composites as measured from stress-strain curves are summarised in Table 1: these values represent the average of measurements from at least five tensile specimens. The apparent tensile modulus, E_0, was determined as mentioned above from the reload portion of several unload/reload cycles conducted after elongation strains between 0.05 and 0.1 %. The 0.2% yield stress for these materials should not be considered a global yield point, since significant micro-yielding in the matrix is apparent from the very beginning of tensile loading.

Engineering stress-strain curves to fracture for the Al_2O_3/Al and B_4C/Al composites are given in Fig. 2. For comparison, the tensile response for the matrix metal (i.e., unreinforced aluminium) processed analogously to the composites is also depicted in the same strain range (the matrix strain to fracture exceeds 20%).

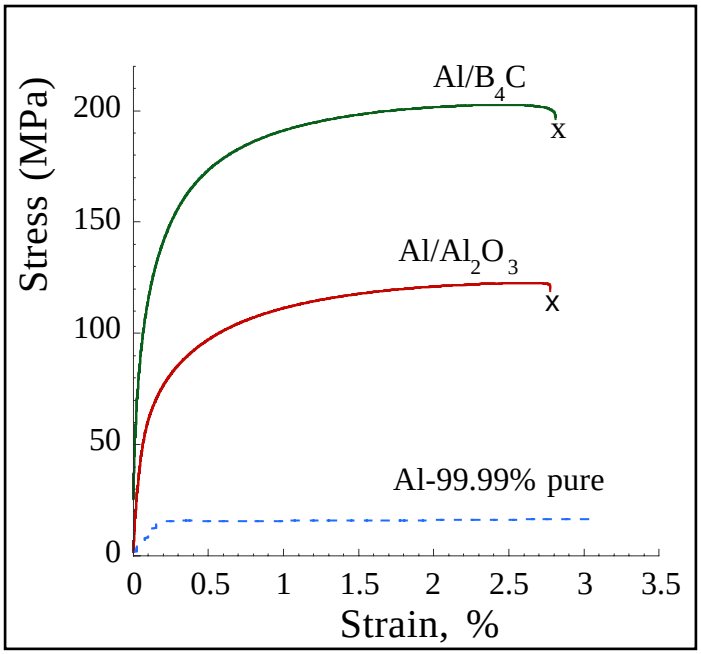

Fig. 2: Characteristic stress-strain curves of the two composite systems

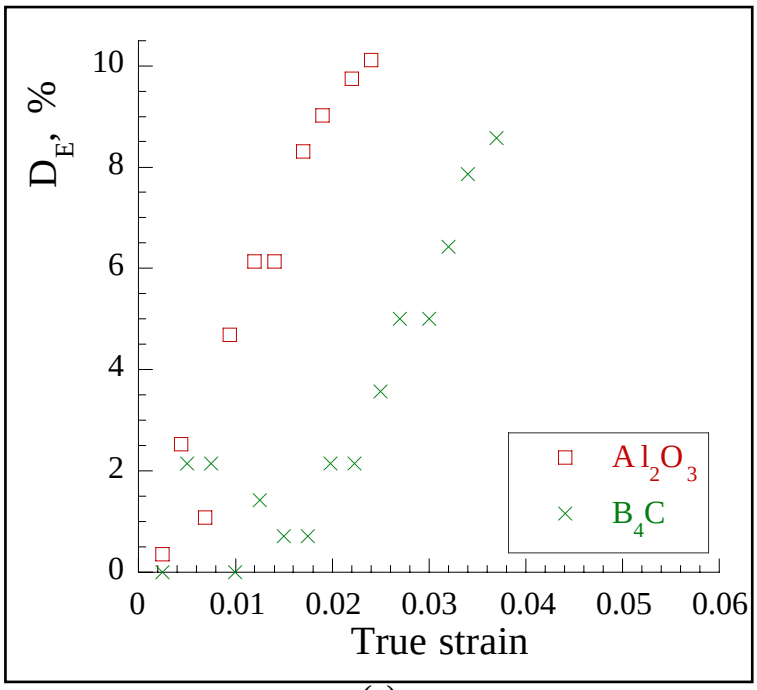

(a)

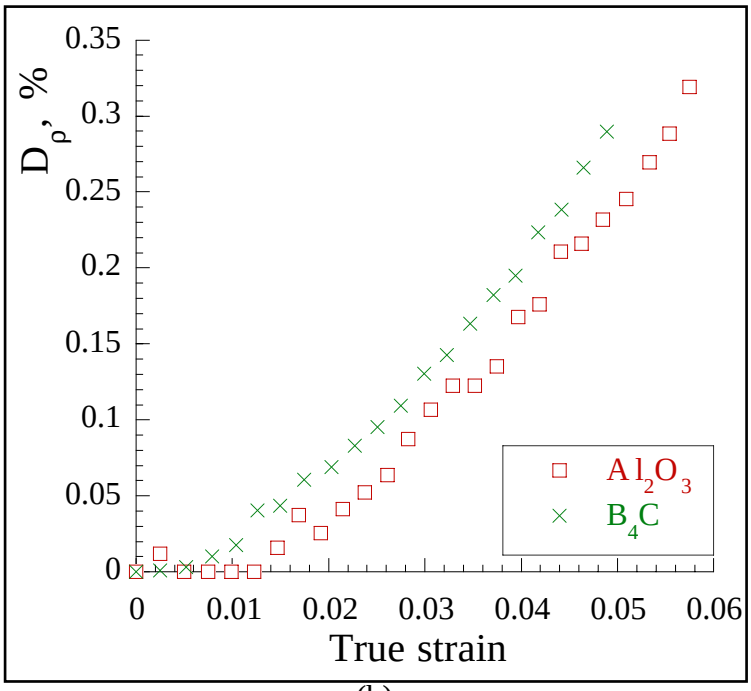

(b)

Fig. 3: Damage evolution as measured by (a) Young's Modulus degradation and (b) density decrease

Damage

The damage parameter as determined from strain-induced degradation of Young's Modulus, D_E, is classically defined as [6]

$$D_E = 1 - E/E_0 \quad (1)$$

where E_0 is the initial Young's modulus of the composite and E is the instantaneous modulus measured after each unloading. In damage mechanics [6] D_E, is taken to characterise the

surface, or volume, fraction of voids, albeit only in a geometrical sense and with no true physical meaning. In contrast, the density-derived damage parameter, D_ρ, is a direct measure of void content and is defined as

$$D_\rho = 1 - \rho/\rho_0 \qquad (2)$$

where ρ_0 is the initial density of the composite and ρ is the instantaneous density after each level of plastic straining. Measured values of D_E and D_ρ are presented in Figs. 3a and 3b, respectively, for the Al/Al_2O_3 and Al/B_4C composites. Damage evolution is apparent in both of the studied systems; however, there is a clear distinction in their response to straining, indicating a difference in the micromechanisms of damage between the two materials.

It was also observed that unload/reload cycles used to measure damage significantly increase the total strain the material can sustain before fracture, roughly from 2.5 to 5 % total elongation, as can be noted by comparison of Figs. 2 and 3.

Damage micromechanisms

In the Al/Al_2O_3 composite, metallographic examination reveals that damage takes two forms: (i) particle fracture which is the dominant damage mode, and (ii) matrix voiding. Matrix voiding is predominantly a consequence of particle fracture, since matrix voids nucleate at the intersection of a particle crack and the matrix-particle interface. Typical micrographs of damage in this material are shown in Figure 4.

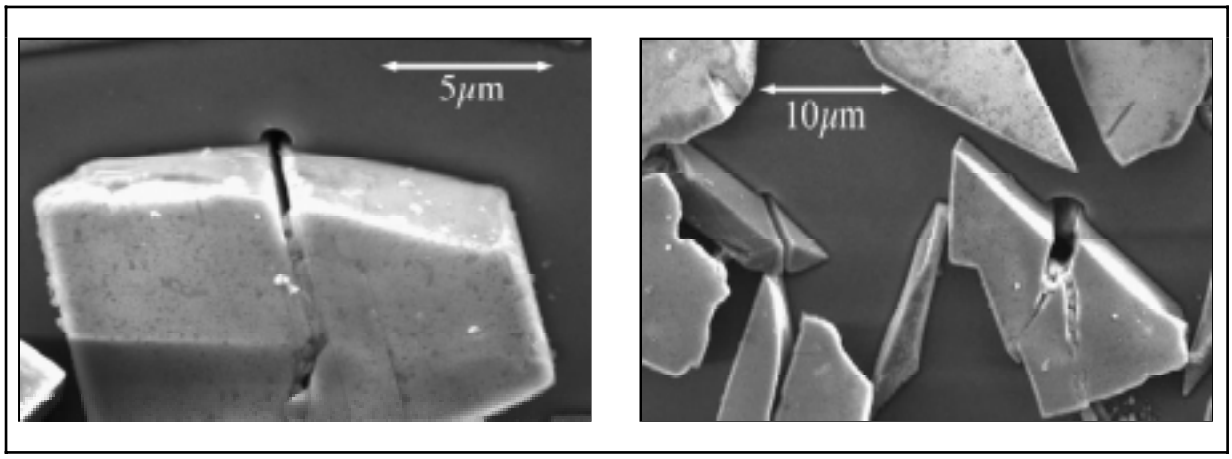

Fig. 4: Damage in the Al_2O_3/Al composite.

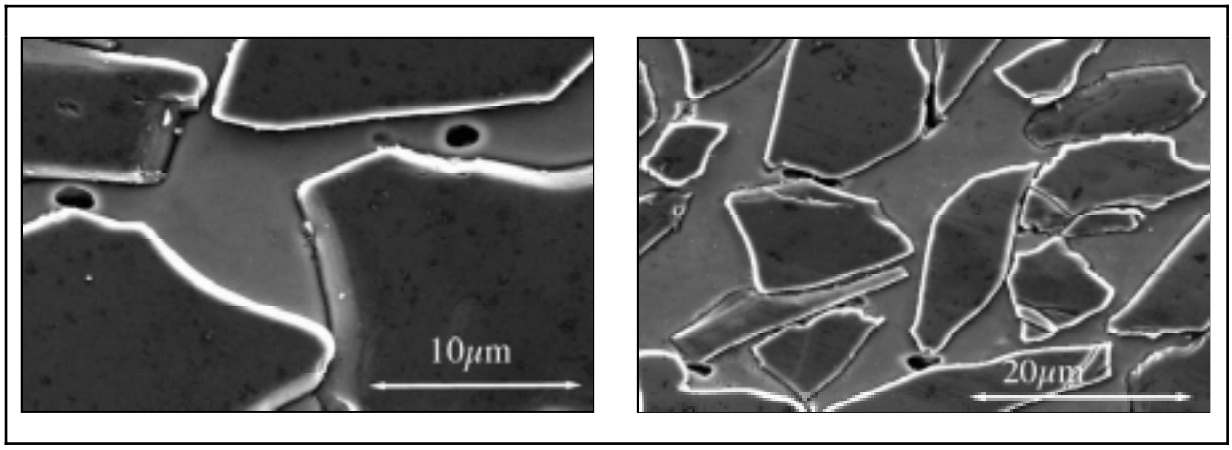

Fig. 5: Damage in the B_4C/Al composite.

Damage in the Al/B_4C composite is in the form of matrix voids, most often nucleated at or near the particle-matrix interface. Micrographs show these voids in matrix regions that seem to be highly constrained mechanically by the particles, Fig. 5. A few fractured particles were also observed in the boron carbide composites very close to the fracture surface; however, their frequency was considerably less than in alumina-reinforced composites.

DISCUSSION

The Hashin-Shtrikman bounds for the elastic modulus of the two composites are given in Table 2, together with the value predicted by a three-phase self consistent generalised scheme [7]. Comparison with the experimental values, obtained as described above from unload/reload cycles at low plastic strain, reveals that measured values are below the Hashin-Shtrikman lower bound for both composites. This could be due to (i) localised matrix plasticity at all stages of the reload curve, or (ii) a rapid build-up of damage in the composites in the early stages of initial straining. The former explanation would imply that no truly elastic composite deformation stage existed during unload/reload cycles, presumably due to a highly inhomogeneous stress-strain distribution in the two phases. Work is in progress on the issue.

The damage parameter, D_E, increases as deformation progresses for both composites. There is a similar increase in the density-based damage parameter D_ρ; however, these two damage parameters differ by one to two orders of magnitude. This is expected: even in a homogeneous elastic solid, D_E exceeds D_ρ by a factor between two and four [8-10]. In the present materials, the observation that, D_E exceeds D_ρ by a significantly larger factor must be a result of damage accumulation in regions of the composites which carry a high proportion of the load: namely the particles, and matrix regions of high triaxiality. That this ratio would be higher in the Al_2O_3/Al composite, where damage takes the form of cracked particles, as compared to the B_4C/Al composite where damage predominantly takes the form of matrix voiding, stands to reason since the stiff particles carry the major portion of the load.

Table 2: Elastic moduli of component phases of the composites, and calculated for the composite by the Hashin-Shtrikman bounds, and a three-phase self-consistent scheme.

	Young's Modulus,E (GPa)	Poisson's Ratio
Boron Carbide (B_4C) [11]	445	0.17
Aluminium Oxide (Al_2O_3) [11]	400	0.27
Aluminium (Al)	70	0.345
50% B_4C/Al:		
Hashin-Shtrikman lower bound	153	0.21
Self consistent three-phase model	159	0.28
Hashin-Shtrikman upper bound	211	0.31
50% Al_2O_3/Al:		
Hashin-Shtrikman lower bound	147	0.26
Self consistent three-phase model	152	0.30
Hashin-Shtrikman upper bound	193	0.34

Measured tensile elongations at fracture for both composite systems exceed 2.5%. These values are high for a material that is about 50% by volume ceramic: published data on pressure-infiltrated aluminium matrix composites reinforced with particles above 10 μm in diameter seldom show elongations that exceed 1% [12-14]. Ductile materials exhibit plastic instability that can be predicted using the Considère criterion, which in the case of damage accumulating materials, as the ones studied, can be written in the form:

$$\frac{d\sigma}{d\varepsilon} = \sigma \left(1 - \frac{1}{1 - D_\rho} \frac{dD_\rho}{d\varepsilon}\right) \qquad (3)$$

where σ is the true (macroscopic) flow stress of the damaging material, ε is the true strain, and D_ρ is the density-based damage parameter as defined above. For the values of D_ρ and $dD_\rho / d\varepsilon$ measured in this study the term in brackets of Eqn. (3) is close to one and can be ignored. The flow curves and their derivative are presented in Fig. 5, where good agreement is evident between the data and Considère's criterion. Hence, we can conclude that the elongations achieved in these materials are as high as can be expected given their flow stress and rate of work hardening, implying that fracture is not defect-controlled. Similar agreement between data and Considère's criterion was observed in prior work on particle reinforced aluminium, albeit for materials with much lower volume fractions ceramic (approximately 15%) [15].

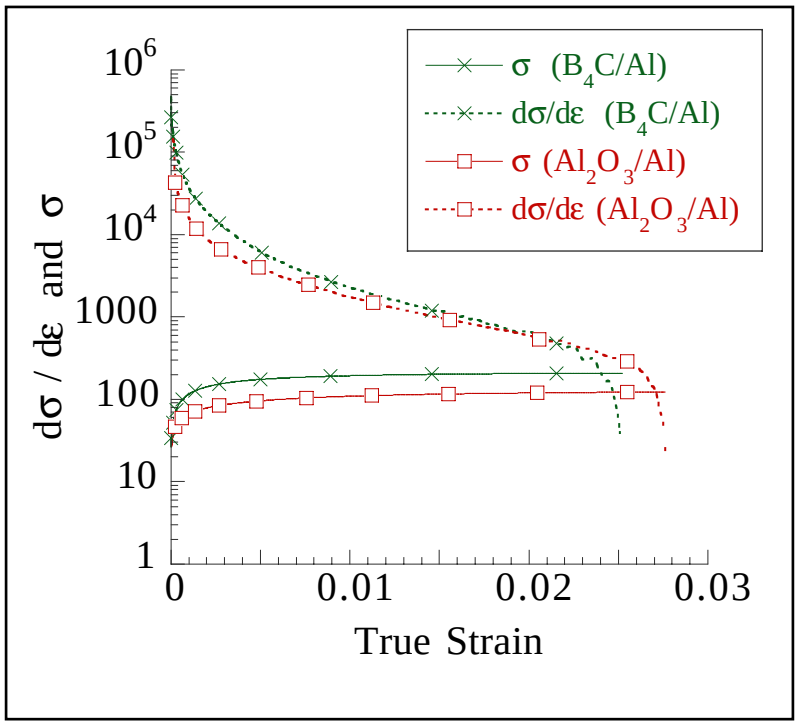

Fig. 5: Tensile curves and their derivative for the Al_2O_3/Al and B_4C/Al composites.

The flow curves of the two materials resemble one another; however, the flow stress for the boron carbide reinforced composite exceeds that of the composite reinforced with aluminium oxide by about 75 MPa (Fig. 2 and Table 1). The matrix is the same, as are the size and coefficients of thermal expansion of the reinforcing phases in both composites; hence the matrix flow stress is expected to be similar. The different flow behaviour of the two composites must, therefore, be a consequence of differences in the intrinsic mechanical behaviour of the two reinforcements. Since the difference in stiffness between boron carbide and alumina is relatively small (Table 2), the difference between the two flow curves must result from the fact that alumina particles fracture from the very beginning of the loading

process, whereas boron carbide particles remain mostly intact. This observation and its interpretation are in agreement with data of Vaidya et al. [16], who compared quasi-static tensile responses of SiC/Al and B_4C/Al composites containing about 15 vol. pct reinforcement. They found that the flow stress is higher and that the propensity for particle failure is lower, in the B_4C composite compared with the SiC reinforced material. These observations underscore the significant differences that exist between the different ceramic reinforcing particles that can be used to produce metal matrix composites.

CONCLUSIONS

- Al_2O_3/Al and B_4C/Al composites can be produced by pressure gas infiltration featuring defect-free homogeneous microstructures with 50% by volume of reinforcement phase.

- Total elongations to failure of 2.5% have been measured for both composites during monotonic loading.

- The ultimate tensile strengths of the Al_2O_3/Al and B_4C/Al composites are around 120 and 200 MPa respectively, showing a strong influence of the reinforcement on the tensile behaviour.

- Microstructural observations of failed tensile samples indicate that damage in the Al_2O_3/Al composite accumulates primarily by particle fracture, whereas damage in the B_4C/Al composite accumulates predominantly by matrix voiding.

- Two methods were used to measure the evolution of internal damage in the composites during tensile deformation: (i) degradation of Young's modulus, and (ii) decrease in density. The measurements reveal different trends that can be correlated with the micromechanisms of damage in the two materials.

ACKNOWLEDGEMENTS

The authors acknowledge funding from the Swiss National Science Foundation, project No. 2100-049119.96. Many thanks are extended to Dr. Bernard Viguier for assistance with the TEM work. In addition, the authors would like to thank Mr. Ali Miserez and Dr. Andreas Rossoll for contributing many engaging discussions and comments.

REFERENCES

1. A.M. Murphy:*Clustering in Particulate Metal matrix Composites,* Ph.D. thesis, Cambridge,1997.

2. P. Poza and J.Llorca, "Fracture Toughness and Fracture Mechanisms of Al-Al_2O_3 Composites at Cryogenic and Elevated Temperatures", *Materials Science and Engineering,* vol. A206, 1996, pp. 183-193.

3. D.J. Lloyd, "Particle reinforced aluminium and magnesium matrix composites", *International Materials Reviews,* vol. 39, 1994, pp. 1-24.

4. J.A. Isaacs, F. Taricco, V.J. Michaud, and A. Mortensen, "Chemical Stability of Zirconia-Stabilized Alumina Fibers During Pressure Infiltration by Aluminum", *Metallurgical Transactions,* vol. 22A, 1991, pp. 2855-2862.

5. R.T. Ratcliffe, "The Measurement of Small density Changes in Solids", *British Journal of Applied Physics*, vol. 16, 1965, pp. 1193-1196.

6. J. Lemaitre, *A course on Damage Mechanics*, Springer-Verlag, Berlin, 1992.

7. R.M. Christensen, *Mechanics of Composite Materials,* Wiley-Interscience Publication, New York, 1979, pp. 32-58.

8. W.D. Kingery, H.K. Bowen, and D.R. Uhlman, *Introduction to Ceramics,* Second Edition, John Wiley & Sons, New York, 1976.

9. J.K. Mackenzie, "The Elastic Constants of a Solid Containing Spherical Holes", *Proceedings of the Royal Society of London*, vol. B63, 1950, pp. 2-11.

10. J.B. Wachtman: in *Mechanical Properties of Ceramics,* Wiley-Interscience Publication, New York, 1996, pp. 409.

11. Engineered Ceramics Handbook, *Ceramics and glasses,* ASM International, Materials Park, 1991.

12. J. Yang, C. Cady, M.S. Hu, F. Zok, R. Mehrabian, and A.G. Evans, "Effects of Damage on the Flow Strength and Ductulity of a Ductile Al Alloy Reinforced with SiC Particulates", *Acta Metallurgica et Materialia*, vol. 38, 1990, pp. 2613-2619.

13. R.H. Pestes, S.V. Kamat, and J.P. Hirth, "Effect of Microstructural Parameters on the Yield Strength of Al-4%Mg/Al_2O_3p Composites", *Scripta Metallurgica et Materialia,* vol. 30, 1994, pp. 963-967.

14. J. Yang, S.M. Pickard, C. Cady, A.G. Evans, and R. Mehrabian, "The Stress/Strain Behavior of Aluminum Matrix Composites with Discontinuous Reinforcements", *Acta Metallurgica et Materialia*, vol. 39, 1991, pp. 1863-1869.

15. C. Gonzales and J. Llorca, "Prediction of the Tensile Stress-Strain Curve and Ductility in Al/SiC Composites", *Scripta Materialia,* vol. 35, 1996, pp. 91-97.

16. R.U. Vaidya, S.G. Song, and A.K. Zurek, "Dynamic Mechanical Response and Thermal Expansion of Ceramic Particle Reinforced Aluminium 6061 Matrix Composites", *Philosophical Magazine,* vol. A 70, 1994, pp. 819-836.